RADIO FREQUENCY BASED HEART RATE VARIABILITY MONITORING

Fengyu Wang, Xiaolu Zeng, Chenshu Wu, Beibei Wang and K. J. Ray Liu

University of Maryland, College Park, MD 20742, USA
Origin Wireless Inc., Greenbelt, MD 20770 USA

ABSTRACT

Heart rate variability (HRV), which measures the fluctuation of heartbeat intervals, has been considered as an important indicator for general health evaluation. In this paper, we present mmHRV, a contact-free HRV monitoring system using commercial millimeter-wave (mmWave) radio. We devise a *heartbeat signal extractor*, which can optimize the decomposition of the phase of the channel information modulated by the chest movement, and thus estimate the heartbeat signal. The exact time of heartbeats is estimated by finding the peak location of the heartbeat signal while the inter-beat intervals (IBIs) can be further derived for evaluating the HRV metrics. Experimental results show that mmHRV can measure the HRV accurately with 3.68ms average error of mean IBI (w.r.t. 99.49% accuracy) based on the experiments over 10 participants.

***Index Terms*—** Heart rate variability (HRV), heartbeat estimation, wireless sensing, millimeter-wave radio.

1. INTRODUCTION

Heart rate variability (HRV), defined as the variation of the periods between consecutive heartbeats, i.e., inter-beat intervals (IBI), is an important indicator of the overall health status of an individual [1]. Traditional measurements of the HRV are obtained by continuously measuring the IBIs using dedicated medical devices such as electrocardiogram (ECG) or photoplethysmogram (PPG) sensors, which are cumbersome for daily use. Therefore, how to monitor the HRV in a non-contact way has become an important topic.

Radio frequency (RF) based sensing has been regarded as one of the most promising techniques because the presence of a human object will affect the RF signal propagation. RF signals reflected from the human body will be modulated by the body movement such as the chest movement caused by respiration and heartbeat. Therefore, vital signs of the human subject can be unveiled by analyzing the channel propagation characteristics [2–7].

As an early attempt of non-contact vital sign monitoring, ViMo [8] tries to accurately estimate the heart rate (HR) of users using commodity millimeter wave radio, but it leaves plentiful information unaddressed for HRV estimation. In this work, we present a subsequent work - mmHRV, aimed at non-contact HRV estimation using a single COTS millimeter wave radar. Technically, accurate HRV estimation is much more difficult than HR estimation. The existing HR estimating systems usually try to accumulate samples in the time domain to achieve higher HR estimation accuracy [8–12]. However, they are not applicable for HRV estimation which needs the exact time of each heartbeat.

Note that the respiration movement ranges from $4-12$mm with a frequency of $6 - 30$ breaths per minute (BPM) [13] while the heartbeat movement ranges from $0.2 - 0.5$mm with a frequency of $50 - 120$ BPM, both of which are quasi-periodic signals. Given such an intrinsic feature, we develop a *heartbeat signal extractor*, which optimizes the decomposition of the composite signal with several band-limited signals. Among the decomposed signal components, the heartbeat wave will be the one whose amplitude and frequency satisfy the requirement of a typical heartbeat signal. The peaks of the estimated heartbeat wave are picked to identify the exact time of each heartbeat, and the IBIs can be further derived for calculating several HRV metrics.

The rest of the paper is organized as follows. Section 2 presents the theoretical model of CIR measurements. The details of the heartbeat extractor and HRV estimation are introduced in Section 3 while the experimental evaluation is discussed in Section 4. Section 5 concludes the paper.

2. THEORETICAL MODELING OF CIR MEASUREMENTS

mmHRV builds upon a commodity frequency-modulated continuous-wave (FMCW) radar [14] which transmits a series of waveforms called chirps, with the pulse repetition time (PRT) T_s. The duration of each chirp signal is T_c, where $T_c < T_s$. The frequency of the chirp signal increases linearly with time and the transmitting signal is denoted as

$$x_T(t) = A_T \exp\{-j[2\pi f_c t + \pi \frac{B}{T_c} t^2]\}, \tag{1}$$

for $t \in [0, T_c]$, where A_T is the transmitting power, f_c is the chirp starting frequency and B is the bandwidth. When the electromagnetic (EM) wave is reflected by the human chest at

distance $d(t)$, the reflected signal $x_R(t)$ can be expressed as

$$x_R(t) = A_R \exp\{-j[2\pi f_c(t-t_d) + \pi \frac{B}{T_c}(t-t_d)^2]\}, \quad (2)$$

where A_R is the amplitude of the receiving signal. t_d stands for the round-trip delay and can be denoted as $t_d = \frac{2d(t)}{c}$, where c is the speed of light. Mixing the received signal with a replica of the transmitted signal and following a low-pass filter, the channel information $h(t)$ can be expressed as

$$h(t) = A \exp\{-j(2\pi \frac{Bt_d}{T_c}t + 2\pi f_c t_d - \pi \frac{B}{T_c}t_d^2)\}. \quad (3)$$

Note that the term $\pi \frac{B}{T_c}t_d^2$ is negligible, especially in short-range scenarios. Therefore, the $h(t)$ can be written as

$$h(t) = A \exp\{-j(2\pi \frac{Bt_d}{T_c}t + 2\pi f_c t_d)\}, \quad (4)$$

which is a sinusoidal signal whose frequency $f_b \triangleq \frac{Bt_d}{T_c} = \frac{2Bd(t)}{cT_c}$ depends on the target's distance.

For simplicity, we denote the channel information for chirp m as $h_m(t) \triangleq h(t - mT_s)$, where $m = \lfloor t/T_s \rfloor$. For each chirp, the baseband signal $h_m(t)$ is digitized by ADC, producing N samples per chip, referred to as fast time. As the frequency of $h_m(t)$ relates to the distance of reflecting point, the channel impulse response (CIR) can be obtained by performing Range-FFT, where

$$h(r,m) = \sum_{n=0}^{N-1} h_m(n) \exp\{-j2\pi rn/N\}. \quad (5)$$

Here we assume the reflected signal falls into the r_0-th range bin, then the CIR in Equ. (4) can be rewritten as

$$h_{r_0}(m) = \tilde{h}_{r_0} \exp\{2\pi f_c t_d(m)\}, \quad (6)$$

where the common phase shift is absorbed in $\tilde{h}_{r_0}$, and we can observe that the phase of the CIR measurement changes periodically in slow time due to the periodic motions of respiration and heartbeat.

3. HEARTBEAT EXTRACTION AND HRV ESTIMATION

Estimating HRV requires accurate estimation of inter-heartbeat intervals (IBIs), therefore, we need to extract the displacement change caused by heartbeats (a.k.a., heartbeat wave) from the compound displacement change of chest wall and detect moments in which heartbeats occur.

3.1. Heartbeat Extraction Algorithm

Recall that the phase information reflects the distance change caused by vital signs. For simplicity, we directly use the analog form of signals, and the distance change of the human chest can be written as

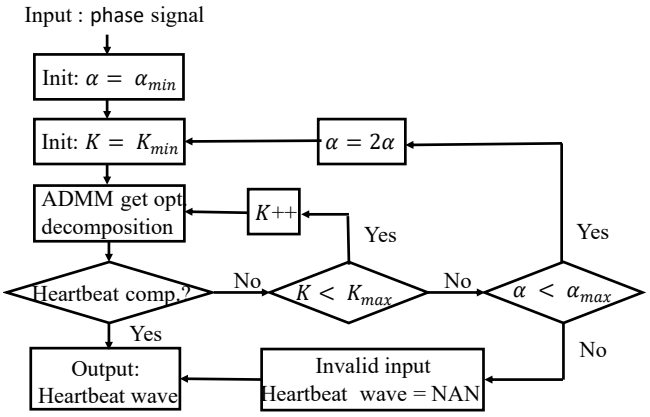

Fig. 1: Processing flow of heartbeat wave extraction.

$$y(t) = s_m(t) + s_r(t) + s_h(t) + n(t), \quad (7)$$

where $s_m(t)$ denotes the distance change caused by body motion. $s_r(t)$ and $s_h(t)$ denote the distance change caused by respiration and heartbeat, respectively. $n(t)$ is the random phase offset introduced by noise, which is independent with the phase change caused by vital signs.

Note that both $s_r(t)$ and $s_h(t)$ are quasi-periodic signals, where the period can slightly change over time. Besides, we assume the body motion introduces few oscillations, i.e., a base-band signal. Thus, the signals related with the human subject are sparse in the spectral domain and we can reconstruct these signals with a few band-limited signals. In specific, each component $u_k(t)$ is assumed to be compact around a center pulsation ω_k, which is to be determined along with the decomposition. Moreover, the decomposition should satisfy the spectrum sparsity and data fidelity requirements at the same time, which is modeled as

$$\min_{u_k \in \mathcal{U}, \omega_k \in \Omega} \alpha \sum_{k=1}^{K} \left\| \partial t \left[(\delta(t) + \frac{j}{\pi t}) * u_k(t) \right] \exp(-j\omega_k t) \right\|_2^2 + \left\| y(t) - \sum_{k=1}^{K} u_k(t) \right\|_2^2, \quad (8)$$

where the first term evaluates the bandwidth of the analytic signal associated with each component, and the second term evaluates the data fidelity. K is the total number of decomposition components, where $\mathcal{U} = \{u_1(t), \ldots, u_K(t)\}$ and $\Omega = \{\omega_1, \ldots, \omega_K\}$ are the set for all components and their center frequencies, respectively. α is a parameter for balancing the bandwidth constraint and data fidelity.

Once the hyper-parameters are known, the optimization problem in Equ. (8) can be solved by alternatively updating

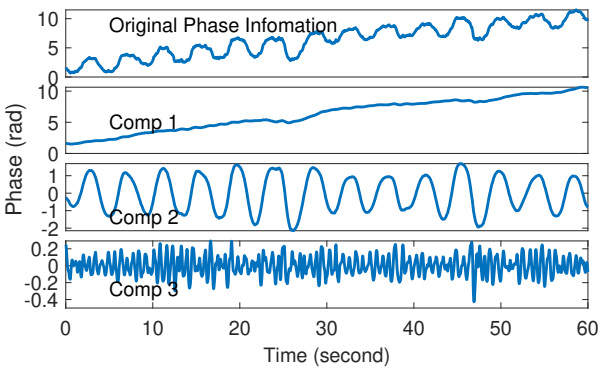

(a) Decomposition of a typical phase signal in time domain

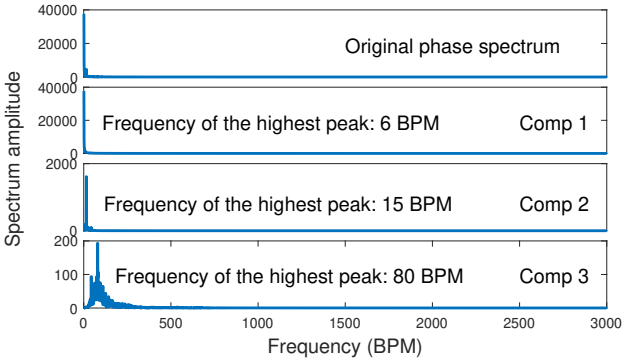

(b) Corresponding spectrum of the decomposed component

Fig. 2: Example of heartbeat extractor. (a) is the decomposition result in time domain, (b) is the corresponding spectrum of each component. In this example, the 1st component corresponds to body motion, the 2nd component corresponds to respiration and the 3rd component corresponds to heartbeat.

$u_k(t)$ and ω_k until convergence, i.e. ADMM algorithm [15]. The minimizer of the Equ. (8) w.r.t. $u_k(t)$ is [16],

$$\sqcap_k(\omega) = \frac{\dagger(\omega) - \sum_{i,i\neq k} \sqcap_i(\omega)}{1 + 2\alpha(\omega - \omega_k)^2}, \tag{9}$$

where $\sqcap_k(\omega)$ and $\dagger(\omega)$ are the Fourier transfer of $u_k(t)$ and $y(t)$ respectively. Besides, the minimizer of the Equ. (8) w.r.t. ω_k is

$$\omega_k = \frac{\int_0^\infty \omega|\sqcap_k(\omega)|^2 d\omega}{\int_0^\infty |\sqcap_k(\omega)|^2 d\omega}. \tag{10}$$

However, it is hard to predefine these hyper-parameters in real applications for heartbeat wave extraction. First, the human motion does not always exist and the human respiration sometimes will have a strong second harmonic component, making it even harder to determine the component number. Furthermore, the hyper-parameter α also influences the decomposition performance by adjusting the balance between bandwidth constraint and data fidelity.

In mmHRV, to accurately decompose the signal and get the heartbeat wave, we are trying to adaptively change the component number K and α for different datasets, as shown in Fig. 1. The system tries to get the estimate of heartbeat wave with relative small predefined K and α. If the decomposed components do not contain the heartbeat signal, the hyper-parameter K increases to avoid the mode mixing problem. Considering that only a limited number of sources consist the composite phase signal, there is an upper-bound for the component number K. When the hyper-parameter K exceeds the upper-bound and the system still does not get a good estimate of the heartbeat signal, the hyper-parameter α increases to further avoid mode mixing problem. The upper-bound of α is predefined to save the computation time, and the algorithm will terminate either when the heartbeat signal is successfully decomposed or both α and K exceed the upper-bound. Thanks to the selection of location bins w.r.t. human chest before heartbeat signal extraction, where the selected phase signal should exhibit periodicity and its variance should fall in a predefined range (i.e., SINR constraint), we do not observe the decomposition failure case in the experimental evaluation.

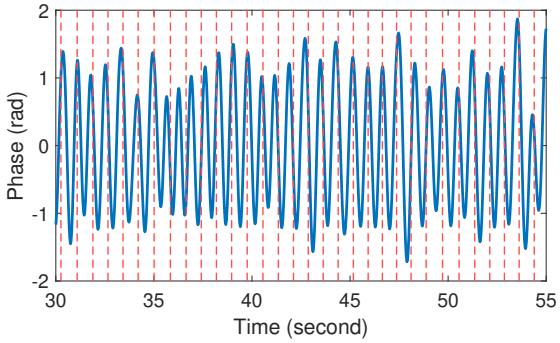

Fig. 3: Example of IBI estimation. The ground-truth from ECG are marked as dashed lines.

Fig. 2 illustrates the decomposition of a typical one-minute phase signal from the experiment, where the original phase information has been decomposed into 3 components. The first component reflects the body motion of the human subject, the second component is the respiration motion, and the third component is the heartbeat wave. The spectrum of each component is shown in Fig. 2 (b).

3.2. HRV Estimation

Once the heartbeat wave is extracted, the exact time corresponding to each heartbeat can be identified by the peaks of the heartbeat wave. To further increase the accuracy, normalization is performed before peak extraction. IBIs can thus be derived by calculating the time duration between two adjacent heartbeats. Fig. 3 shows a segment of heartbeat wave

Table 1: HRV estimation results in terms of mean IBI, RMSSD and SDRR for 10 subjects.

Metrics	Methods		User ID									
			1	2	3	4	5	6	7	8	9	10
Mean IBI	Value (ms)	ECG	899.4	789.9	723.2	854.6	654.5	645.2	890.1	564.9	728.1	763.8
		mmHRV	906.3	790.4	725.6	848.6	652.4	644.2	888.1	574.2	722.7	762.6
		BPFB	881.5	784.2	781.5	842.1	676.6	651.5	878.4	579.1	719	773.5
	Error (ms)	**mmHRV**	6.95	0.45	2.47	5.92	2.17	0.99	1.97	9.33	5.38	1.2
		BPFB	17.87	5.7	58.36	12.44	22.01	6.31	11.66	14.21	9.16	9.66
RMSSD	Value (ms)	ECG	38.59	10.85	37.56	31.49	34.05	16.88	27.52	5.26	23.28	31.16
		mmHRV	33.52	16.53	39.08	35.26	20.29	18.14	26.06	27.8	30.52	34.92
		BPFB	59.34	54.26	53.83	52.94	78.57	95.09	45.56	140.36	59.61	47.92
	Error (ms)	**mmHRV**	5.08	5.68	1.52	3.77	13.76	1.26	1.46	22.53	7.25	3.76
		BPFB	20.75	43.41	16.27	21.45	44.53	78.21	18.04	135.1	36.34	16.76
SDRR	Value (ms)	ECG	56.28	22.91	50.54	35.35	33.61	23.24	32.66	12.25	35.83	50.87
		mmHRV	43.22	27.25	53.3	45.88	33.54	25.49	37.43	38.66	37.15	45.51
		BPFB	71.01	47.28	110.29	58.92	69.68	67.61	50.44	118.41	47.92	63.94
	Error (ms)	**mmHRV**	13.07	4.34	2.76	10.53	0.07	2.24	4.78	26.42	1.31	5.36
		BPFB	14.72	24.37	59.74	23.57	36.07	44.37	17.78	106.16	12.09	13.07

and its ECG ground-truth, where the dashed lines show the exact time of each heartbeat from a commercial ECG sensor [17]. The peaks of normalized heartbeat wave match with the ground-truth, as shown in Fig. 3.

The HRV features can be further obtained from the IBI sequence. In mmHRV, we use the two most widely used metrics to evaluate the HRV [18]. One is the root mean square of successive differences (RMSSD), which measures the successive IBI changes, and can be calculated by

$$\mathrm{RMSSD} = \sqrt{\frac{1}{N_{\mathrm{IBI}}-1}\sum_{i=2}^{N_{\mathrm{IBI}}}(\mathrm{IBI}(i)-\mathrm{IBI}(i-1))^2}, \quad (11)$$

where N_{IBI} is the total number of IBIs of the measurement. The other one is SDRR, which measures the standard deviation of all the IBIs, can be calculated as

$$\mathrm{SDRR} = \sqrt{\frac{1}{N_{\mathrm{IBI}}}\sum_{i=1}^{N_{\mathrm{IBI}}\mathrm{IBI}}(\mathrm{IBI}(i)-\overline{\mathrm{IBI}})^2}, \quad (12)$$

where $\overline{\mathrm{IBI}}$ is the empirical mean of the IBIs.

4. EXPERIMENTAL EVALUATION

In this section, we evaluate the performance of mmHRV, where 10 participants (5 male and 5 female) aging from 20 to 60 are enrolled for testing. To further evaluate the performance of the proposed system, we compare mmHRV with the state-of-the-art HRV estimation technique using band-pass-filter-bank (BPFB) [19], where the heartbeat signal is estimated by using the narrow BPF whose passing band contains HR.

Table. 1 shows the estimated HRV features in terms of mean IBI, RMSSD and SDRR of 10 participants, where the distance between user and device is 1m. It is shown that mmHRV can achieve 3.68ms average error of mean IBI, 6.61ms average error of RMSSD and 7.09ms average error of SDRR. Correspondingly, the average estimation error of BPFB is 16.73ms of mean IBI, 43.09ms of RMSSD and 35.19ms of SDRR. We can see that mmHRV outperforms BPFB for all the 3 metrics. This is because that mmHRV directly extracts the heartbeat signal from the composite signal by optimizing the decomposition, so that the error propagation from breathing as well as random body motion elimination can be avoided. Besides, the accurate heart rate estimation is necessary for BPFB method, which however is vulnerable to noise and interference from other signal components.

5. CONCLUSION

In this paper, we develop mmHRV to estimate HRV using CIR measured by a commercial millimeter wave radar. The heartbeat wave is estimated by decomposing the composite phase signal concurrently to avoid the error propagation issue compared to the state-of-art work. Experiment results show the potential of the proposed system for contactless HRV estimation with high accuracy.

6. REFERENCES

[1] U. Rajendra Acharya, K. Paul Joseph, N. Kannathal, C. M. Lim, and J. S. Suri, "Heart rate variability: a review," *Medical and biological engineering and computing*, 2006.

[2] K. J. R. Liu and B. Wang, *Wireless AI: Wireless Sensing, Positioning, IoT, and Communications*, Cambridge University Press, 2019.

[3] E. Cianca, M. De Sanctis, and S. Di Domenico, "Radios as sensors," *IEEE Internet of Things Journal*, 2017.

[4] B. Wang, Q. Xu, C. Chen, F. Zhang, and K. J. R. Liu, "The promise of radio analytics: A future paradigm of wireless positioning, tracking, and sensing," *IEEE Signal Processing Magazine*, 2018.

[5] F. Wang, F. Zhang, C. Wu, B. Wang, and K. J. Ray Liu, "Respiration tracking for people counting and recognition," *IEEE Internet of Things Journal*, 2020.

[6] F. Zhang, C. Wu, B. Wang, M. Wu, D. Bugos, H. Zhang, and K. J. R. Liu, "SMARS: Sleep monitoring via ambient radio signals," *IEEE Transactions on Mobile Computing*, 2019.

[7] C. Chen, Y. Han, Y. Chen, H. Lai, F. Zhang, B. Wang, and K. J. R. Liu, "TR-BREATH: Time-reversal breathing rate estimation and detection," *IEEE Transactions on Biomedical Engineering*, 2018.

[8] F. Wang, F. Zhang, C. Wu, B. Wang, and K. J. R. Liu, "Vimo: Multi-person vital sign monitoring using commodity millimeter wave radio," *IEEE Internet of Things Journal*, 2020.

[9] F. Adib, H. Mao, Z. Kabelac, D. Katabi, and R . C. Miller, "Smart homes that monitor breathing and heart rate," in *Proceedings of the 33rd Annual ACM Conference on Human Factors in Computing Systems*, 2015.

[10] Z. Yang, P. H. Pathak, Y. Zeng, X. Liran, and P. Mohapatra, "Monitoring vital signs using millimeter wave," in *Proceedings of the 17th ACM International Symposium on Mobile Ad Hoc Networking and Computing*, 2016.

[11] M. Mercuri, I. R. Lorato, Y. Liu, F. Wieringa, C. Van Hoof, and T. Torfs, "Vital-sign monitoring and spatial tracking of multiple people using a contactless radar-based sensor," *Nature Electronics*, 2019.

[12] A. Ahmad, J. C. Roh, D. Wang, and A. Dubey, "Vital signs monitoring of multiple people using a fmcw millimeter-wave sensor," in *2018 IEEE Radar Conference (RadarConf18)*, 2018.

[13] A. De Groote, M. Wantier, G. Cheron, M. Estenne, and M. Paiva, "Chest wall motion during tidal breathing," *Journal of Applied Physiology*, 1997.

[14] TI Inc, "TI product," `https://www.ti.com/product/IWR1843`, 2020, [Online; accessed 23-August-2020].

[15] Stephen Boyd, Neal Parikh, and Eric Chu, *Distributed optimization and statistical learning via the alternating direction method of multipliers*, Now Publishers Inc, 2011.

[16] K. Dragomiretskiy and D. Zosso, "Variational mode decomposition," *IEEE Transactions on Signal Processing*, 2014.

[17] BITALINO Inc, "Bitalino Revolution Plugged Kit BT," `https://bitalino.com/en/plugged-kit-bt`, 2020, [Online; accessed 23-August-2020].

[18] F. Shaffer and J. P. Ginsberg, "An overview of heart rate variability metrics and norms," *Frontiers in public health*, 2017.

[19] V. L. Petrovic, M. M. Jankovic, A. V. Lupsic, V. R. Mihajlovic, and J. S. Popovic-Bozovic, "High-accuracy real-time monitoring of heart rate variability using 24 ghz continuous-wave doppler radar," *IEEE Access*, 2019.